

EDN: STKJDD

УДК 532.6

Secondary Destruction of Organic Coal-water Slurry Drops at Different Temperatures in a Gas Flow

Anna A. Shebeleva*

Alexander V. Shebelev†

Andrey V. Minakov‡

Anastasia K. Okrugina§

Siberian Federal University
Krasnoyarsk, Russian Federation

Received 29.05.2024, received in revised form 04.06.2024, accepted 14.07.2024

Abstract. A computational study of the secondary destruction of a drop of organic water-coal fuel (OCWS) in a gas flow was carried out. For the first time, the influence of the temperature of an OCWF drop, which has non-Newtonian properties, on deformation and its further destruction was studied. The computational study was carried out using a numerical technique based on the VOF method, the LES model was used to take into account turbulence, and the technology of adapted dynamic meshes was used to describe the behavior of the interface on the main turbulent scales, which made it possible to resolve secondary liquid droplets up to 20 μm in size. During the work, the shape of the surface of an OCWF drop during the destruction process, as well as the structure of the flow near and in the wake of the drop, were studied. As a result of the calculations, the dependences of the rate of transverse deformation of the midsection of an OCWF drop for different temperatures were obtained. Judging by the results, with increasing temperature, the destruction time of an OCWF drop decreases, which has a beneficial effect on the mixing of OCWF with air.

Keywords: OCWS fuel, secondary destruction of a drop, deformation rate, mathematical modeling, dynamic mesh adaptation technology.

Citation: A.A. Shebeleva, A.V. Shebelev, A.V. Minakov, A.K. Okrugina, Secondary Destruction of Organic Coal-water Slurry Drops at Different Temperatures in a Gas Flow, J. Sib. Fed. Univ. Math. Phys., 2024, 17(5), 654–664. EDN: STKJDD.



Introduction

Currently, special attention is paid to the socio-economic development of the northern and Arctic regions. This is due to the presence in these regions of large reserves of natural resources, such as non-ferrous metal ores, gas, oil and coal. Since coal production has been increasing recently, coal fuel will remain one of the main energy sources in the near future. However, we should not forget about environmental problems that arise when burning coal, such as emissions of nitrogen oxides and carbon dioxide into the atmosphere. To reduce harmful effects on atmosphere and environment during energy production, it is proposed to use alternative fuels, such

*an_riv@mail.ru <https://orcid.org/0000-0001-6126-9757>

†Ashebelev@sfu-kras.ru

‡Aminakov@sfu-kras.ru

§okrugina_a02@mail.ru

© Siberian Federal University. All rights reserved

as coal-water fuel (CWF), consisting of water and coal dust, or organic water-coal fuel (OCWF), consisting of water, crushed coal (or combustible waste from its processing), a small amount of chemical additives (for example, surfactants, plasticizers) and a petroleum combustible component (waste oil) [1]. To burn liquid waste of petroleum origin in its original state, large resources are needed; according to data [2], waste of petroleum origin and waste oils form masses amounting to millions of tons per year and require further disposal. However, as part of OCWF, these wastes can be used to intensify ignition and improve rheological characteristics of fuel [3]. Use of by-products from coal mining and oil refining industries as part of OCWF can help eliminate waste from these industries and reduce the harmful impact of energy sector on nature. Also, the advantages of using OCWF include the absence of dust and contamination during storage, transportation and use of fuel. Today, there are technologies for industrial preparation and combustion of CWF in furnaces of power boilers, experimental methods and numerical modeling algorithms have been developed, and practical recommendations have been formulated for the combustion of CWF droplets [4–7]. China and Japan are already using CFC combustion on an industrial scale. The works [3, 8–10] describe stages of preparation and ignition of OCWF droplets. To date, data on the maximum ignition and combustion temperatures are presented for a narrow composition of OCWF, which also complicates the process of studying these types of fuels. The problem of ignition and combustion of OCWF is not simple, this is due to fact that OCWF is multicomponent, contains solid particles, and this fuel most often has non-Newtonian properties. To increase the efficiency of fuel combustion, its preliminary atomization in combustion chamber is required; the technical task in this case is to optimize the process of destruction of the jet, which includes changing the shape of the surface of the drop and its secondary destruction. The development of an effective method for burning OCWF will allow low-quality fossil fuels to be included in the fuel balance and solve the problem of recycling industrial waste that pollutes the environment, thereby improving the environmental situation by reducing harmful emissions into the atmosphere.

One of first experimental works on study of secondary crushing of OCWF droplets was work [11]. The authors, in work [12], conducted a detailed experimental study of OCWF spray for a coaxial nozzle, obtained quantitative information on characteristics of OCWF atomization (average droplet size, shape and spray angle) with and without fuel treatment for purposes of application in design of combustion chambers gas turbines burning OCWF. Also, a semi-empirical correlation was developed to determine average spray particle sizes as a function of various parameters, including Weber number, Reynolds number, and air-to-fuel mass flow ratio. Heating of OCWF (flash atomization) has been found to be very effective in reducing droplet size not only at atmospheric pressure but also at elevated pressure. A detailed experimental study of fragmentation of individual OCWF droplets was carried out for the first time in the work [13]. The authors studied the morphology of droplets at various Weber numbers, $We = \frac{\rho_g u_g^2 d_0}{\sigma}$ and Ohnesorge numbers, $Oh = \frac{\eta}{\sqrt{\sigma \rho L}}$. Later, in the work [7] a numerical study of behavior of an OCWF drop during secondary crushing was carried out. The results obtained were compared with experimental data on droplet crushing modes considered in the experimental work [7]. Despite the seemingly sufficient number of works in the field of studying OCWF, at the moment there are practically no works related to the numerical study and establishment of the dependence of the shape of the drop surface, deformation, and destruction time on the rheological properties of OCWF [14, 15].

1. Numerical technique for destruction of OCWF droplets

Since one of ways to obtain data on secondary destruction of a fuel droplet is numerical modeling, in our works [16, 17] we proposed and verified a numerical method for the destruction of OCWF droplets. This technique showed good agreement between calculated and experimental data on the destruction of OCWF droplets and the rate of deformation of the droplet. When developing numerical methodology, information about flow structure and physical properties of gas-droplet flows was taken into account. It was also taken into account that fluid under consideration can be either a viscous Newtonian or a non-Newtonian viscoplastic fluid, behaviour of which can be described by one of common rheological models, such as the power-law, Bingham or Herschel-Bulkley model [17] a numerical model was proposed and verified method of destruction of OCWF droplets. To simulate destruction of an OCWF drop, the Ansys Fluent software package was used; the VOF method was used to describe free surface; a detailed description is presented in work [18]. According to this method, the OCWF and air flow are considered as a single two-component medium, and phase distribution within computational domain is determined using marker function $F(x,y,z,t)$. The volume fraction of liquid phase in calculation cell is taken equal to $F(x,y,z,t) = 0$ if cell is empty, $F(x,y,z,t) = 1$ if cell is completely filled with liquid, $0 < F(x,y,z,t) < 1$ if interphase boundary passes through the cell. Tracking movement of interface is performed by solving the equation for transfer of volume fraction of liquid phase in cell:

$$\frac{\partial F}{\partial t} + u_i \frac{\partial F}{\partial x_i} = 0, \quad (1)$$

where: u_i is the velocity vector of a two-phase medium, found from solving a system of hydrodynamic equations: the mass conservation equation or the continuity equation:

$$\frac{\partial \rho}{\partial t} + \frac{\partial}{\partial x_i} (\rho u_i) = 0, \quad (2)$$

and equations of motion or the law of conservation of momentum:

$$\frac{\partial}{\partial t} (\rho u_i) + \frac{\partial}{\partial x_j} (\rho u_i u_j) = \frac{\partial \sigma_{ij}}{\partial x_j} - \frac{\partial p}{\partial x_i} - \frac{\partial \tau_{ij}}{\partial x_j} + F_{s_i}, \quad (3)$$

here τ_{ij} is the subgrid stress tensor, F_s is vector of body forces, p is static pressure, ρ is density of two-phase medium. Components of viscous stress tensor σ_{ij} :

$$\sigma_{ij} \equiv \left[\mu \left(\frac{\partial u_i}{\partial x_j} + \frac{\partial u_j}{\partial x_i} \right) \right] - \frac{2}{3} \mu \frac{\partial u_i}{\partial x_i} \delta_{ij}, \quad (4)$$

where: μ is dynamic viscosity of two-phase medium. Density and Newtonian viscosity of two-component medium under consideration are found through volume fraction of liquid in cell according to the mixture rule:

$$\rho = \rho_1 F + (1 - F) \rho_2, \quad (5)$$

$$\mu = \mu_1 F + (1 - F) \mu_2, \quad (6)$$

where: ρ_1, μ_1 – density and viscosity of liquid, ρ_2, μ_2 – density and viscosity of gas. The obtained values of density ρ and viscosity μ are included in equations of motion and determine physical properties of two-phase medium.

To simulate destruction of droplets, special attention must be paid to surface tension, in this case, the CSF algorithm [19] was used, which involves introducing into equations of motion an additional body force F_s , value of which is determined from relation:

$$F_s = \sigma k \nabla F, \quad (7)$$

where: σ is surface tension coefficient, k is curvature of free surface, which is defined as the divergence of normal vector:

$$k = \nabla \left(\frac{n}{|n|} \right). \quad (8)$$

The normal to free surface is calculated, in turn, as the gradient of volume fraction of liquid phase in cell:

$$n = \nabla F. \quad (9)$$

Since turbulent flows are observed during secondary destruction, the LES model was used [20].

$$\tau_{ij} - \frac{1}{3} \tau_{kk} \delta_{ij} = -2\mu_t S_{ij}, \quad (10)$$

$$S_{ij} = \frac{1}{2} \left(\frac{\partial u_i}{\partial x_j} + \frac{\partial u_j}{\partial x_i} \right), \quad (11)$$

where: τ_{ij} is subgrid stress tensor, S_{ij} is strain rate tensor, μ_t is subgrid viscosity. In this work, we used subgrid viscosity model proposed by Smagorinsky:

$$\mu_t = \rho L_s^2 |S|, \quad (12)$$

where: L_s is length of subgrid scale mixing:

$$L_s = \min \left(kd, C_s V^{1/3} \right), \quad (13)$$

$$|S| \equiv \sqrt{2S_{ij}S_{ij}}, \quad (14)$$

here: k is the Karman constant, d is distance to nearest wall, V is volume of the computational cell C_s is the Smagorinsky constant. In this work, the value $C_s = 0.17$ was used.

For modeling properties of OCWF, the Herschel-Bulkley rheological model was used:

$$\mu(\dot{\gamma}) = \frac{k\dot{\gamma}^n + \tau_0}{\dot{\gamma}}. \quad (15)$$

where: $\dot{\gamma}$ is shear rate, τ_0 is yield strength of the viscoplastic fluid, n is flow index, k is fluid consistency index.

For modeling destruction of droplets, including very small ones, special attention should be paid to computational mesh. During secondary destruction of OCWF, small drops are formed, resolution of which is a rather complex process, therefore, the technology of gradient adaptation of the computational mesh is used in proposed numerical technique. According to this technology, during calculation process mesh is automatically condensed in area of large solution gradients, gradient of volume fraction of liquid was chosen as control parameter. At initial moment of time, there are 40 calculated cells per drop along its diameter. In this case, there are at least 8 cells per interface. Total number of computational nodes in optimized mesh during calculation process was close to 12 million nodes.

2. Problem formulation and numerical simulation results

To describe destruction of OCWF droplets in a gas flow, an isothermal formulation of problem was used. OCWF is a water-coal suspension consisting of 60–70% by weight of coal powder, 30–40% water and a small amount of additives. Depending on composition, OCWF can be either a Newtonian or non-Newtonian fluid. In our case, OCWF droplets have non-Newtonian

properties and are described by the Herschel–Bulkley rheology. The physical properties of fuel suspensions under consideration were taken from experimental work [21] (see Tab. 1), where ρ_l is density of OCWF, τ_0 is yield strength of viscoplastic fluid, k is consistency index, n is flow index, σ – coefficient of surface tension of OCWF, T – temperature of OCWF. Air with following properties was considered as a gas: $\rho_g = 1.7 \text{ kg/m}^3$, $\mu_g = 1.789 \cdot 10^{-5} \text{ Pa}\cdot\text{s}$. The computational domain is a parallelepiped with dimensions $0.026 \times 0.026 \times 0.08 \text{ m}$. On one of faces of parallelepiped, an entry condition with a fixed velocity value was set, and on remaining faces of computational domain, free exit conditions were set. At initial moment of time, at a distance of 0.0015 m from entrance of computational domain, a spherical drop of OCWF with an initial diameter of $d_0 = 0.003 \text{ m}$ was placed, which was affected by an air flow with a speed of $u_g = 50 \text{ m/s}$ and deformed drop.

Table 1. Physical properties of OCWF fuel suspensions

T, K	ρ_l , kg/m ³	τ_0 , Pa	k , Pa*s ⁿ	n	σ , N/m	We
278	1063	47.08	0.66	1	0.247	51.6
298	1062	37.36	0.42	1	0.239	53.3
308	1061	26.57	0.39	1	0.231	55.2
318	1059	16.99	0.32	1	0.223	57.2

The secondary disintegration of an OCWF drop occurs under influence of an aerodynamic force exceeding surface tension forces. Quantitatively, ratio of these forces is determined by the Weber number. Value of the Weber number determines regime of destruction of drop.

For developing new fuel combustion technologies or burning fuel at low temperatures (e.g. in Arctic conditions), its preliminary atomization in combustion chamber is important to increase contact surface of fuel with the oxidizer. Main task in fuel atomisation and further improvement of combustion technologies is to determine induction time of destruction, shape of surface and rate of deformation of droplet at different times.

In Fig. 1 shows regimes of destruction of an OCWF drop at different temperatures, interval between pictures is $\Delta t = 500 \mu\text{s}$. In Fig. 1a you can see process of deformation of an OCWF drop at a temperature of 278 K, time of interaction of drop with flow is $11000 \mu\text{s}$. At such a low temperature, drop does not collapse for a long time; a process of deformation and flattening of drop in a plane normal to gas flow velocity vector is observed. At a time of $\approx 8500 \mu\text{s}$, central part of drop begins to thin out and stretch along flow, upon reaching a time of $11000 \mu\text{s}$, complete destruction of central part of drop is observed.

When the OCWF temperature increases to 298 K, pattern of droplet deformation changes (Fig. 1b). Interaction time of the drop with flow is $6000 \mu\text{s}$. Initially, spherical drop at time instant $\approx 2000 \mu\text{s}$ resembles shape of a "disk". Over time, the central part of the "disk" inflates like a "parachute"; this is clearly visible at time $\approx 5500 \mu\text{s}$. This regime of destruction for a Newtonian liquid was described in detail in the work [22], authors write that this regime of destruction for Newtonian liquids exists in the range of Weber numbers from 12 to 50. In this case, when destruction of a non-Newtonian drop of OCWF at temperature 298 K, Weber number is $We = 53.3$.

In Fig. 1c shows pictures of destruction of a drop of OCWF at a temperature of 308 K. The drop is destroyed according to a scenario close to previous case (see Fig. 1 b). However, if in case of Fig. 1b, destruction of the "parachute" is observed at $\approx 5500 \mu\text{s}$, but in this case destruction

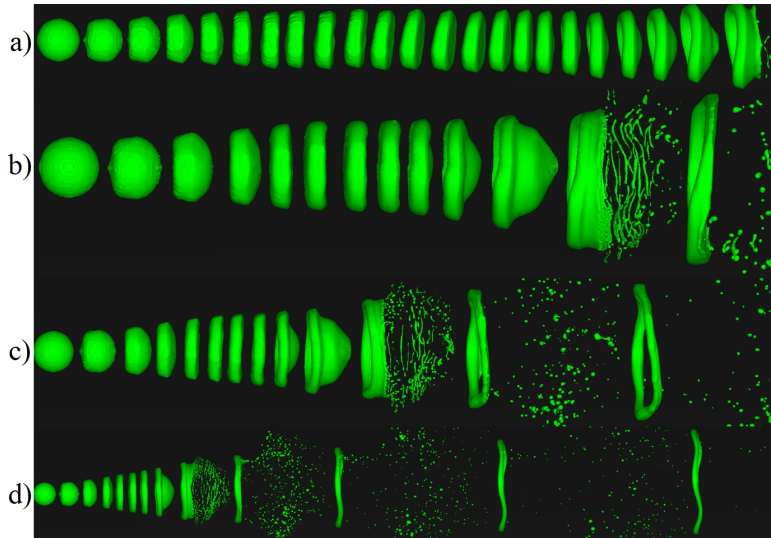


Fig. 1. Regimes of destruction of a drop of OCWF at different temperatures. Interval between frames $\Delta t = 500 \mu s$. a) $t = 278 \text{ K}$, period $0 - 11000 \mu s$; b) $t = 298 \text{ K}$, period $0 - 6000 \mu s$; c) $t = 308 \text{ K}$, period $0 - 6000 \mu s$; d) $t = 318 \text{ K}$, period $0 - 6000 \mu s$

occurs earlier, at $\approx 5000 \mu s$. As can be seen, even with such a small increase in temperature of the OCWF drop from 298 K to 308 K, process of destruction of drop increases in time. Change in the surface shape of an OCWF droplet at a temperature of 318 K is shown in Fig. 1d. The interaction time of a drop with a flow is $6000 \mu s$. In this case, tendency for destruction time to depend on the initial temperature of drop remains unchanged. Destruction of the "parachute" occurs at a time equal to $\approx 4000 \mu s$. Further, shell of central part of OCWF drop is destroyed with formation of small drops; at moment of time $\approx 5000 \mu s$, only a ring remains from initial drop, which subsequently becomes thinner and destroyed.

In course of mathematical modeling, formation of a ring and its further movement along flow was obtained for following OCWF temperatures of 298 – 318 K. After the "parachute" is destroyed, only a ring remains from initially spherical drop, which over time increases in diameter and becomes thinner. For the case of an OCWF droplet with a low temperature of 278 K, we observe formation of a ring, but it thins out so slowly that the computational region was not enough to record complete destruction of droplet. However, for this study this is not important, because we are studying moment of induction of destruction, and not the late stage of interaction of drop with the flow.

The most important indicator of droplet destruction is not only dynamics of deformation, presented in Fig. 1, but also induction time of destruction of the OCWF droplet. Fig. 2 shows pictures of destruction of a drop at a temperature of 278 K at various times. As can be seen, at the moment of time $10377 \mu s$ the central part of drop has already thinned out, but remains intact, and at moment of time $10465 \mu s$ a violation of integrity of shell is already observed, it follows that the OCWF droplet at a temperature 278 K begins to collapse at a time equal to $t_1 \approx 10421 \mu s$. Based on Fig. 1a, Fig. 2, drop was deformed for a long time, and after reaching destruction induction time, central part of drop quickly collapsed.

In Fig. 3 shows dynamics of destruction of a drop of OCWF at a temperature of 298 K in

frontal projection. This type of destruction differs from previous case in that there is a gradual destruction of central part of the drop with a simultaneous thinning of edge of drop - appearance of a ring that increases until it collapses. Induction time of destruction in this case is $t_2 \approx 4955 \mu\text{s}$. Fig. 3 clearly shows that drop begins to collapse from central part. At moment of time $\approx 5006 \mu\text{s}$ the "parachute" has become so thin that streams break off from drop, which increase and break up into small drops. At time $\approx 5560 \mu\text{s}$, complete destruction of central part of drop is observed, liquid ring has increased in size, but has not yet become thin enough to collapse.

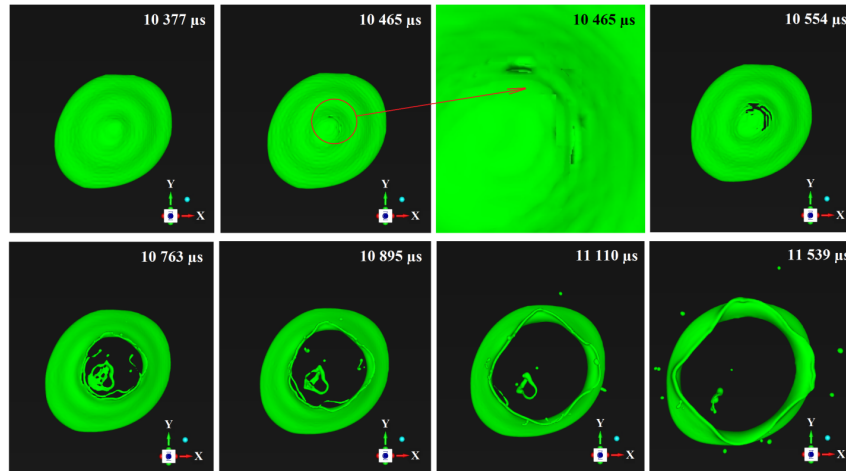


Fig. 2. Frontal projection of destruction of an OCWF drop at $t = 278 \text{ K}$

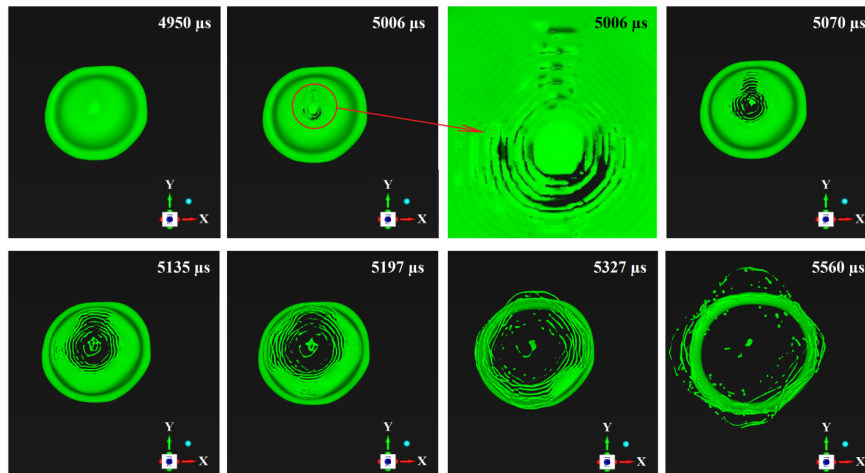


Fig. 3. Frontal projection of destruction of an OCWF drop at $t = 298 \text{ K}$

Fig. 4 shows moments of destruction of an OCWF drop at a temperature of 308 K. Induction time of destruction in this case is $t_3 \approx 4463 \mu\text{s}$. If we compare results obtained in Fig. 4 with results presented in Fig. 3, we see that with increasing temperature destruction process begins to proceed faster. Thus, at a temperature of 298 K (Fig. 3), a drop of OCWF began to collapse

at time instant $\approx 4955 \mu\text{s}$. And at a temperature of 308 K (Fig. 4) at same point in time, we observe that the central part of the drop has already been completely destroyed and only a liquid ring remains.

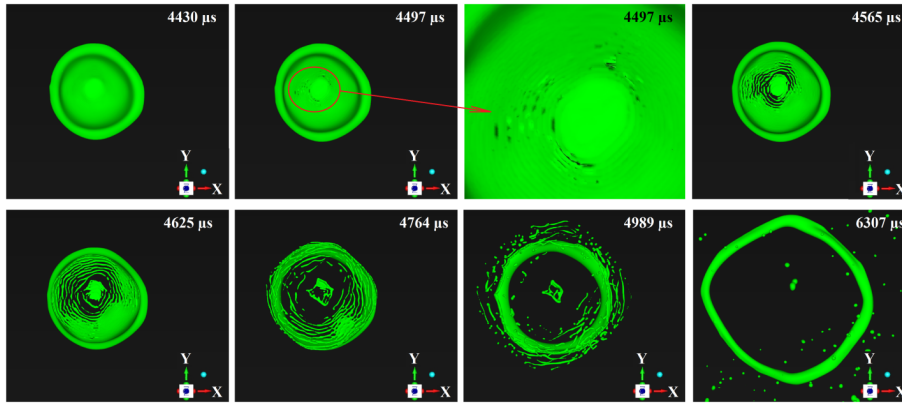


Fig. 4. Frontal projection of destruction of an OCWF drop at $t = 308 \text{ K}$

The scenarios for destruction of an OCWF drop at temperatures of 298–318 K are very similar: gradual transverse stretching of the drop along midsection until drop resembles shape of a "disk", further thinning of central part of drop and its inflation in a "parachute" type, destruction of "parachute" into small drops and as a result, a ring remains from original drop, which becomes thinner and collapses. In this case, destruction begins at time $t_4 \approx 3598 \mu\text{s}$, this can be seen from Fig. 5.

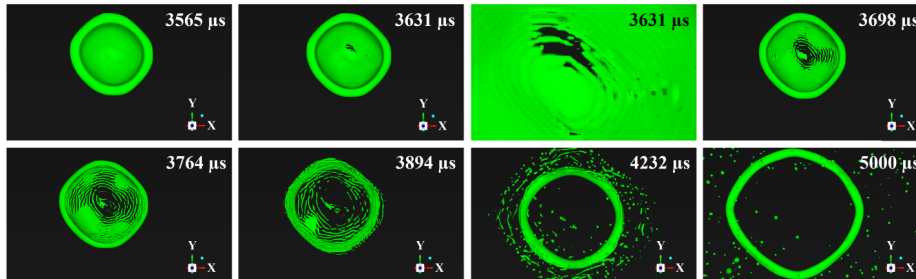


Fig. 5. Frontal projection of destruction of an OCWF drop at $t = 318 \text{ K}$

For quantitative assessments of destruction of droplet surface shape, dependence of ratio of maximum value of droplet midsection to initial size d_0 is used, where d_{max} is maximum size of droplet shape during the deformation process, at a moment in time. This dependence is also called rate of transverse deformation of the drop (Fig. 6).

Based on results (Fig. 6), as temperature of the OCWF drop increases, ratio of maximum deformation of drop to initial size increases. Also, for the first time, estimates were made of the influence of temperature of an OCWF drop on induction time of destruction and rate of deformation of drop at moment of destruction. Thus, with increasing temperature, destruction time of an OCWF droplet decreases, and ratio of maximum deformation of droplet to initial size

increases. Quantitative calculation indicators, such as the induction time of destruction and ratio of maximum deformation of drop to initial size at moment of destruction are presented in Tab. 2.

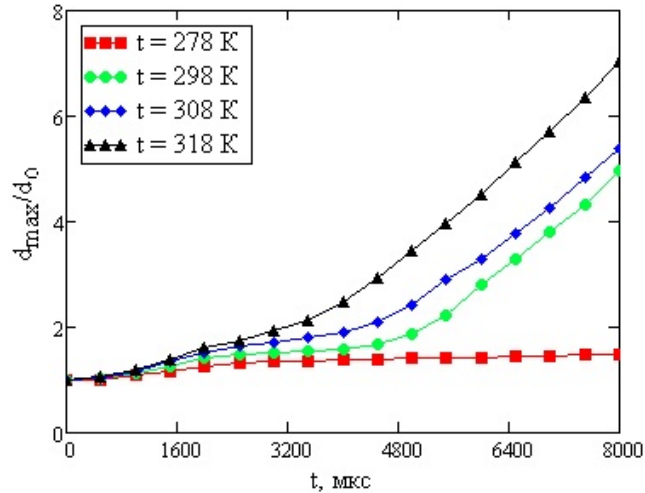


Fig. 6. Rate of transverse deformation of an OCWF drop at different fuel temperatures

Table 2. Quantitative results of destruction of a drop of OCWF

OCWF temperature, T, K	Induction time of destruction, t, μ s	d_{max}/d_0
278	10421	1.798
298	4955	1.874
308	4463	2.069
318	3598	2.185

Conclusion

A computational study of secondary destruction of a drop of organic-coal fuel in a gas flow was carried out in order to improve its combustion technologies. Droplets with different initial temperatures from 278 to 318 K were studied.

The results of numerical modeling have yielded images of destruction of OCWF droplets. These images demonstrate that fuel drops, which have non-Newtonian properties and are described by the Herschel–Bulkley rheology, deform according to the "parachute" scenario within the studied temperature range. At the same time, for a temperature close to freezing and equal to 278 K, the drop is deformed for a long time before collapsing. This is due to fact that at such low temperatures fuel has a higher yield strength, as well as a higher surface tension coefficient. At the initial temperature of the OCWF drop equal to 318 K, the drop is destroyed much more intensely. Induction time of destruction is reduced by approximately 3 times (compared to a temperature of 278 K), which has a beneficial effect on mixing of OCWF with air.

Dependences of induction time of destruction and rate of transverse deformation of drop on initial temperature of the OCWF drop obtained in work will be useful for improving technology of combustion of OCWF, including in regions of the Far North.

The reported study was carried out with the support of the "Krasnoyarsk Regional Fund for Support of Scientific and Scientific-Technical Activities" within the framework of the scientific project "Study of the characteristics of secondary crushing of coal water slurries containing petrochemicals in order to improve technologies for its combustion in Arctic conditions" no. 20231113-06407.

References

- [1] A.Kijo-Kleczkowska, Combustion of coal-water suspensions, *Fuel*, **90**(2011), 865–877.
- [2] BP, BP Statistical Review of World Energy, *London: BP* , **90**(2015), 48.
- [3] G.S.Khodakov, E.G.Gorlov, Suspension coal fuel, *Chemistry of solid fuel*, **6**(2005), 15–32 (in Russian).
- [4] V.I.Murko, V.I.Fedyaev, et al., Investigation of the spraying mechanism and combustion of the suspended coal fuel, *Thermal Science*, **19**(2015), 243–251.
DOI: 10.2298/TSCI120618095M
- [5] A.P.Burdukov, A.A.Emel'yanov, V.I.Popov, S.N.Tarassenko, An investigation of the rheology and dynamics of combustion of composite coal-water slurries, *Thermal Engineering.*, **44**(1997), 492–497.
- [6] Z.Gao, S.Zhu, M.Zheng, Z.Wu, H.Lu, W.Liu, Effects of fractal surface on rheological behavior and combustion kinetics of modified brown coal water slurries, *International Journal of Coal. Science and Technology*, **2**(2015), 211–222. DOI: 10.1007/s40789-015-0075-0
- [7] S.M.Tavangar, H.Hashemabadi, A.Saberimoghadam, CFD simulation for secondary breakup of coal-water slurry drops using OpenFOAM, *Fuel Processing Technology*, **132**(2015), 153–163. DOI: 10.1016/j.fuproc.2014.12.037
- [8] S.C. Yao, Burning of suspended coal-water slurry droplet with oil as combustion additive, *Combustion and Flame*, **66**(1986), 87–89.
- [9] N.I.Fedorova, Yu.F.Patrakov, V.G.Surkov, A.K.Golovko, Analysis of the combustion character of composite fuels obtained by the cavitation method, *Bulletin of the Kuzbass State Technical University*, **4**(2007), 38–41 (in Russian).
- [10] K.Svoboda, et al., Fluidized bed gasification of coal–oil and coal–water–oil slurries by oxygen–steam and oxygen–CO₂ mixtures, *Fuel Processing Technology*, **95**(2012), 16–26.
DOI: 10.1016/j.fuproc.2011.11.001
- [11] M.Kurmangaliev, V.Nekrasov, Breakup of water-coal slurry drops in air flows, *Fluid Mech. Sov. Res.*, **4**(1975).
- [12] T.Yu., et al., Secondary atomization of coal water fuels for gas turbine applications, *MIT Energy Lab Report.*, **88**(1988).
- [13] H.Zhao, et al., Secondary breakup of coal water slurry drops, *Phys. Fluids*, **23**(2011), 113101–113101. DOI: 10.1063/1.3659495

- [14] H.Zhao, et al., Breakup and atomization of a round coal water slurry jet by an annular air jet, *Chemical Engineering Science*, **78**(2012), 63–74. DOI: 10.1016/j.ces.2012.05.007
- [15] H.Zhao, et al., Influence of rheological properties on air-blast atomization of coal water slurry, *J. Non-Newtonian Fluid Mech.*, **211**(2014), 1–15. DOI: 10.1016/j.jnnfm.2014.06.007
- [16] A.A.Shebeleva, A.V.Minakov, M.Yu.Chernetskii, P.A.Strizhach, Deformation of a droplet of an organic water–coal fuel in a gas flow, *J. Appl. Mech. Tech. Phys.*, **59**(2018), no. 4, 653–661. DOI: 10.1134/S0021894418040119
- [17] A.V.Minakov, A.A.Shebeleva, M.Y.Chernetskiy, P.A.Strizhak, R.S.Volkov, Study of the weber number impact on secondary breakup of droplets of coal water slurries containing petrochemicals, *Fuel.*, **254**(2019), 115606–115606. DOI: 10.1016/j.fuel.2019.06.014
- [18] C.W.Hirt, B.D.Nichols, Volume of fluid (VOF) method for the dynamics of free boundaries, *Journal of computational physics*, **39**(1981), 201–226.
- [19] J.U.Brackbill, D.B.Kothe, C.A.Zemach, Continuum method for modelling surface tension, *J. Comput. Phys.*, **100**(1992), 335–354.
- [20] J.Smagorinsky, General Circulation Experiments with the Primitive Equations, I. The Basic Experiment, *Month. Wea. Rev.*, **91**(1963), 99–164.
- [21] G.Lei, L.Junguo, Study on the Influence of Pulping Process on Rheological Properties of Coal Water Slurry, *IOP Conf. Series: Earth and Environmental Science*, **384**(2019), 1–7. DOI: 10.1088/1755-1315/384/1/012107
- [22] S.V.Bukhman, Experimental study of droplet disintegration, *Bulletin of the Academy of Sciences of the Kazakh SSR*, **1**(1954), 38–43 (in Russian).

Вторичное разрушение капли органоводоугольного топлива различной температуры в потоке газа

Анна А. Шебелева

Александр В. Шебелев

Андрей В. Минаков

Анастасия К. Округина

Сибирский федеральный университет
Красноярск, Российская Федерация

Аннотация. Проведено расчетное исследование вторичного разрушения капли органоводоугольного топлива (ОВУТ) в потоке газа. Впервые изучалось влияние температуры капли ОВУТ, обладающей неньютоновскими свойствами, на деформацию и ее дальнейшее разрушение. Расчетное исследование проводилось с помощью численной методики, основанной на ВОФ-методе, для учета турбулентности использовалась ЛЕС-модель, для описания поведения межфазной границы на основных турбулентных масштабах применялась технология адаптированных динамических сеток, которая позволила разрешить вторичные капли жидкости размером до 20 мкм. В ходе работы была исследована форма поверхности капли ОВУТ в процессе разрушения, а также структура потока вблизи и в следе капли. В результате расчетов были получены зависимости темпа поперечной деформации миделя капли ОВУТ для различных температур, судя по результатам, с увеличением температуры время разрушения капли ОВУТ уменьшается, что благоприятно сказывается на перемешивании ОВУТ с воздухом.

Ключевые слова: дифференциальные уравнения, задача Коши, расщепление, устойчивость, сходимость.